which should be cited to refer to this work.

Preparation and characterization of 3-(4,5-ethylenedithio-1,3-dithiol-2-ylidene)naphthopyranone: a luminescent redox-active donor–acceptor compound

Stefan Dolder,[a] Shi-Xia Liu,[a,*] Xavier Guégano,[a] Mihail Atanasov,[b] Claude A. Daul,[c] Claudia Leiggener,[d] Andreas Hauser,[d] Antonia Neels[e] and Silvio Decurtins[a]

[a]*Departement für Chemie und Biochemie, Universität Bern, Freiestrasse 3, CH-3012 Bern, Switzerland*
[b]*Institute of General and Inorganic Chemistry, Bulgarian Academy of Sciences, "Acad. Georgi Bonchev" str. bldg11, 1113 Sofia, Bulgaria*
[c]*Département de chimie, Université de Fribourg, Pérolles, CH-1700 Fribourg, Switzerland*
[d]*Département de chimie physique, Université de Genève, Sciences II, 30 Quai Ernest-Ansermet, CH-1211 Genève 4, Switzerland*
[e]*Institut de Microtechnique, Université de Neuchâtel, Rue Emile Argand 11, CH-2009 Neuchâtel, Switzerland*

Abstract—A new 1,3-dithiol-2-ylidene substituted naphthopyranone **2** has been synthesized and characterized. UV–vis spectroscopic and cyclic voltammetry results, interpreted on the basis of density functional theory, show that **2** displays an intramolecular charge-transfer transition and acts like a donor–acceptor (D–A) system. Furthermore, a weak fluorescence originating from the excited charge-transfer state is observed.

1. Introduction

Naphthalene and especially perylene derivatives are known to exhibit interesting conducting and optical properties and they have found applications, for instance as xerographic dyes or in organic photovoltaic solar cells.[1,2] In most of these compounds, the naphthalene or perylene units act as electron-acceptors, which have, as in the case of naphthalenetetracarboxylic dianhydride (NDA) or naphthaldiimide (NDI), electron affinities in the range of tetracyano-*p*-quinodimethane (TCNQ).[2] Remarkably, the perylene unit by itself is also known as one of the earliest donors used in the preparation of highly conducting organic solids.[3] However, the relative instability of the perylene cation, the low solubility, and the absence of peripheral interactions greatly limit the preparation of conducting materials.[3]

In contrast, tetrathiafulvalene (TTF) and its derivates feature unique π-donor properties and they are successfully used as versatile building blocks for charge-transfer salts, which give rise to a multitude of organic conductors and superconductors.[4,5] Furthermore, the capacity to form persistent

cation radical and dication species upon oxidation, leads to the formation of mixed-valence systems.[5] As a consequence, TTF derivatives are frequently used as donor units in donor–acceptor (D–A) ensembles, which are of prime interest due to their potential applications in molecular electronics and optoelectronics.[6]

The combination or extension of the naphthalene or perylene units with TTF or 1,3-dithiol-2-ylidene moieties is expected to yield materials with interesting donor–acceptor and/or conducting properties. Very recently, dyads and triads containing one or two TTF units covalently linked through a σ-spacer to perylenediimide (PDI) and NDI have been reported.[7,8] The possibility to develop light intensity dependent molecular electronic switches with these systems has already been demonstrated in a porphyrin–PDI–porphyrin triad.[9] In the case of a TTF–PDI dyad, a reversible modulation of the emission fluorescence intensity in solution by either electron or energy transfer has been achieved.[7] This dyad can therefore be considered as a new kind of molecular redox switch with a delayed optical response.[7]

However, to date neither an example of a TTF unit linked by a π-conjugated spacer to a naphthalene or perylene moiety, nor a naphthalene or perylene core extended by 1,3-dithiol-2-ylidene units has been reported. In the latter case, analogous systems such as furano-quinonoid extended TTFs[10]

---

* Corresponding author. Tel.: +41 31 631 4296; fax: +41 31 631 3995; e-mail: liu@iac.unibe.ch

provide the basic synthetic strategy for the preparation of such compounds. Along this line, we describe herein the synthesis and characterization of 1,3-dithiol-2-ylidene substituted naphthopyranone **2**. Structural, spectroscopic, and electrochemical investigations on **2** have been performed and were rationalized on the basis of time-dependent density functional theory (TDDFT).

2. Results and discussion

2.1. Synthesis

Following the procedure for the preparation of furano-quino-noid extended TTFs,[10] compound **2** was obtained in a reasonable yield (54%) from the trimethylphosphite-mediated coupling reaction of 1,8-naphthalic anhydride with 4,5-ethylenedithio-1,3-dithiole-2-thione **1** (Scheme 1). Compound **2** has been fully characterized by NMR, elemental analysis, IR, and MS as listed in Section 4, as well as by single crystal X-ray analysis.
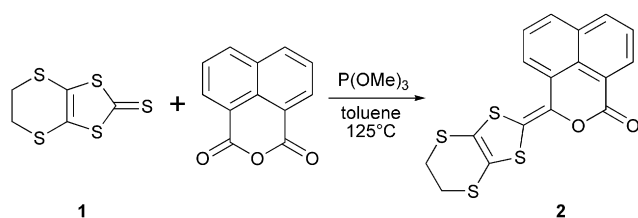
Scheme 1. Synthesis of compound **2**.

2.2. Crystal structure

Compound **2** crystallizes in the monoclinic space group $P2_1$ with one molecule per asymmetric unit. The molecular structure with selected bond distances is shown in Figure 1.

The structural parameters of the planar naphthopyranone unit determined for **2** are comparable with those found for 1,8-naphthalic anhydride.[12] The 4,5-ethylenedithio-1,3-dithiol-2-ylidene entity exhibits a nearly planar geometry
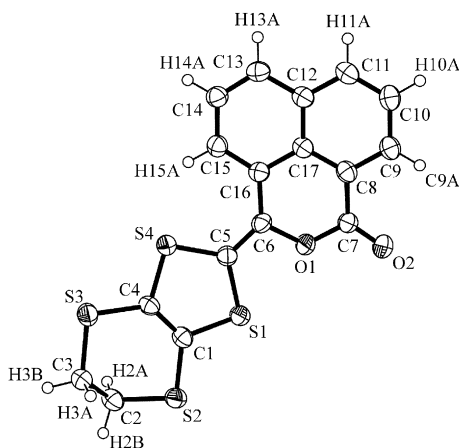

Figure 1. ORTEP[11] representation of the asymmetric unit of **2** (ellipsoids are drawn at 50% probability). Selected bond length [Å]: C5–C6 1.343(7); C5–S1 1.759(5); C5–S4 1.752(5); C6–O1 1.407(6); C7–O1 1.369(6); C7–O2 1.202(6); C1–C4 1.326(7); C1–S1 1.758(5); C4–S4 1.751(5); C1–S2 1.740(5); C4–S3 1.758(4).

typical for this heterocycle in its neutral state.[10a] The whole molecule adopts a conformation, which allows a reduction in steric hindrance between the sulfur atom (S4) of the 1,3-dithiole ring and the hydrogen atom (H15A) of the naphthalene system (interatomic distance S4···H15A is 2.446 Å). The torsion angles C5–C6–C16–C15 and S4–C5–C6–C16 are 12.6° and 2.9°, respectively. Similarly, the bond angles C5–C6–C16 (129.81°) and S4–C5–C6 (125.92°) also reflect this steric repulsion. In the crystal lattice, the molecules are stacked along the *a*-axis in a herringbone type arrangement (Fig. 2). They are linked by some unconventional C–H···O hydrogen bonds but no close S···S contacts can be found.
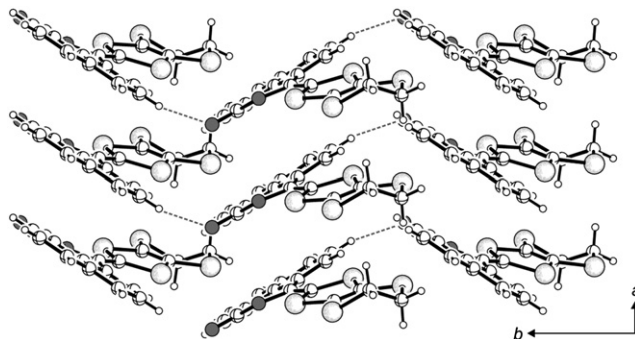

Figure 2. *ab* Projection of the crystal structure of **2**. Stacking of molecules along the *a*-axis in a herringbone type arrangement. Unconventional C–H···O bonds are depicted as dotted lines.

2.3. Electrochemical measurements

The solution redox properties of compound **2** were investigated in dichloromethane by cyclic voltammetry (CV). The cyclic voltammogram is presented in Figure 3. Two quasi-reversible redox processes ($E_{red1}^{1/2}=-1.63$ V, $E_{ox1}^{1/2}=0.74$ V, $\Delta E_{red-ox}=2.37$ V) and one irreversible oxidation ($E_{peak}=1.27$ V) were observed. The first reduction process corresponds to the reduction of the naphthalene unit. The first oxidation process corresponds to the formation of a
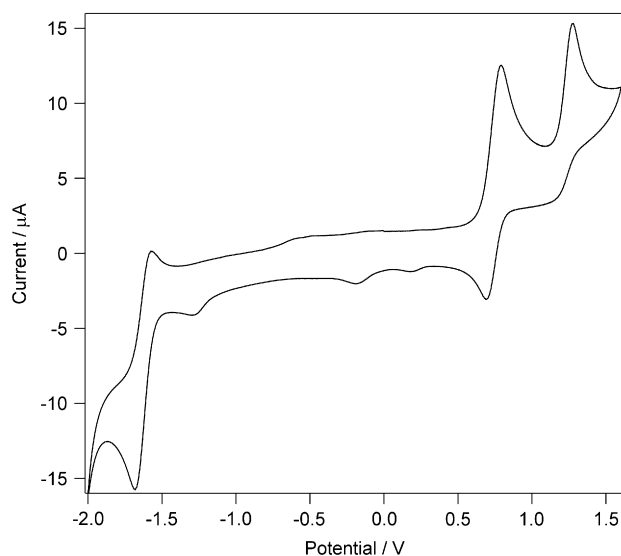

Figure 3. Cyclic voltammogram of **2**, measured under N_2 in CH_2Cl_2 versus Ag/AgCl at room temperature at a scan rate of 100 mV s^{-1}, using 0.1 M Bu_4NPF_6 as electrolyte and Pt as working electrode.

radical cationic species and the second irreversible oxidation correlates with the formation of a thermodynamically unstable dicationic state.

2.4. Photophysical properties and TDDFT calculations

The UV–vis spectrum of **2** shows three strong absorption bands at $33,900 \text{ cm}^{-1}$ (294 nm), $30,800 \text{ cm}^{-1}$ (324 nm), and $21,500 \text{ cm}^{-1}$ (465 nm). In addition, compound **2** shows fluorescence in CH_2Cl_2 with a maximum at $15,700 \text{ cm}^{-1}$ (636 nm) and a quantum yield of around 0.5% at room temperature. In Figure 4, the absorption, luminescence and the corresponding excitation spectra are depicted. The latter agrees well with the absorption spectrum of **2**, suggesting that the fluorescence is indeed due to compound **2** and not due to an impurity or a photoproduct. The large Stokes shift of 5800 cm^{-1}, indicating substantial nuclear rearrangements in the excited state, is in line with the comparatively low quantum yield.
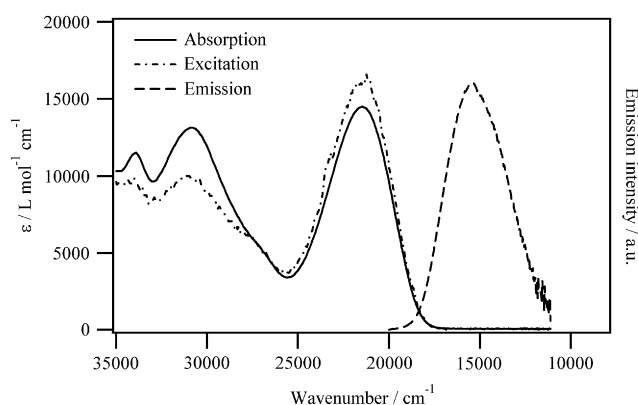

Figure 4. Luminescence (dashed), excitation (dashed-dotted), and absorption (solid) spectra of **2** in CH_2Cl_2 ($c=7.4\times10^{-6}$ M, $\lambda_{ex}=465$ nm, $\lambda_{em}=640$ nm, room temperature).

Moreover, and quite remarkably, the charge-transfer energy calculated from the electrochemical data (Section 2.3) is 2.37 V ($\approx19,100 \text{ cm}^{-1}$), which is almost the same as the zero-point energy of the charge-transfer excited state evaluated from the crossing-point of the absorption and fluorescence spectra ($18,350 \text{ cm}^{-1}$).

Compound **2** can be chemically oxidized to its radical cation **2**$^{\cdot+}$ by $FeCl_3$ or $[Fe(bipy)_3](PF_6)_3$. The decrease of the absorption band at $21,500 \text{ cm}^{-1}$ upon oxidation goes simultaneously with the appearance of new absorption bands at $19,000 \text{ cm}^{-1}$ (526 nm), $15,500 \text{ cm}^{-1}$ (645 nm), and $10,900 \text{ cm}^{-1}$ (917 nm) together with isosbestic points at $20,000 \text{ cm}^{-1}$ and $24,600 \text{ cm}^{-1}$, as shown in Figure 5.

Moreover, in the oxidized form **2**$^{\cdot+}$, the fluorescence is completely quenched.

In order to rationalize the electronic absorption spectrum of **2** and of the oxidized species **2**$^{\cdot+}$, TDDFT calculations with the B3LYP functional were performed for the low-lying excited states. For comparison, excitation energies have been computed both with the experimental geometry of
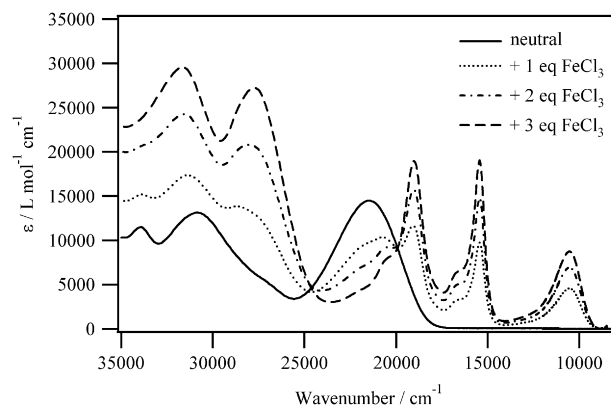

Figure 5. Absorption spectra of **2** in CH_2Cl_2 ($c=2\times10^{-5}$ M) before and after the addition of up to 3 equiv $FeCl_3$.

the neutral **2** and with B3LYP optimized geometries of the neutral and the singly oxidized gas phase species using Ahlichs valence double zeta (VDZ),[13] triple-zeta (TZV) basis sets,[14] and polarization functions[15] with the ORCA[16] implementation of the time-depending DFT method.[17] However, only minor differences could be observed. Therefore, only the excitation energies and absorption intensities of the neutral and the singly oxidized form that have been calculated with the experimental geometry using Ahlichs VDZ basis set[13] are shown in Figure 6 and listed in Table 1. They are in good agreement with the experimental data.

The HOMO of **2** is a π orbital centered on the 1,3-dithiol-2-ylidene subunit, designated in Figure 6 as orbital 95. In contrast, the LUMO of **2** (orbital 96) is more centered on the naphthopyranone subunit. Therefore, the lowest energy transition corresponds to an intramolecular charge-transfer transition.

Another reason that supports the charge-transfer nature of the absorption band at $21,500 \text{ cm}^{-1}$ can be deduced by relating the spectroscopic data with the redox potentials by means of the theory developed by Marcus and Hush.[18,19] This theory correlates a charge-transfer transition with the energetic barrier to thermally activated electron transfer (ΔG^0), which can be estimated from the difference between the redox potentials of the donor and acceptor centers (ΔE_{red-ox}).[19]

The geometric differences for the ground and excited states represent an asymmetric situation, in which the energy of the charge-transfer transition, E_{abs}, is equal to the energy difference between the initial and final states, plus the reorganizational energy λ (Fig. 7, Eq. 1).

$$E_{abs} = \Delta G^0 + \lambda \tag{1}$$

Therefore, a reorganizational energy $\lambda \approx 2400 \text{ cm}^{-1}$ for the absorption band at $21,500 \text{ cm}^{-1}$ can be calculated from the CV data. The energy λ can be correlated to $\Delta\nu_{1/2}$, the bandwidth at half-height of the absorption band, using Eq. 2.[20]

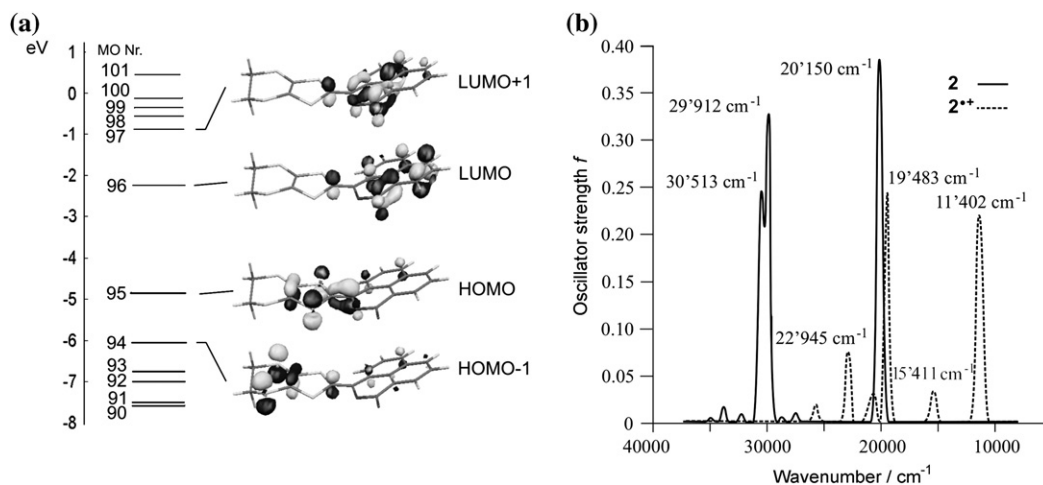$$\Delta\nu_{1/2} = 48.06\lambda^{1/2} \tag{2}$$

3

Figure 6. (a) MO scheme for **2**. The HOMO–LUMO excitation essentially corresponds to an intramolecular charge-transfer transition from the 1,3-dithiol-2-ylidene unit to the naphthopyranone part; (b) electronic transitions for **2** and **2**[·+] calculated by TDDFT,[17] B3LYP functional, Ahlrichs VDZ basis set,[13] and ORCA.[16]

Table 1. TDDFT energies, oscillator strengths (*f*) and assignments of the electronic transitions of **2** (geometry of X-ray structure) and **2**[·+] (adopting the X-ray geometry of **2** without change), B3LYP functional, Ahlrichs SVP basis set,[13] ORCA[16,17]

2				**2**[·+]			
Transition energy (cm^{-1})	*f*	Assignment		Transition energy (cm^{-1})	*f*	Assignment	
20,150 (*21,500*)	0.40	95→96	89%	11,402 (*10,900*)	0.22	*94→95	90%
		95→97	6%			95→96	7%
27,563	0.01	94→96	64%	15,411 (*15,500*)	0.03	*93→95	85%
		95→97	28%			95→96	7%
28,758	0.01	95→98	30%	18,079	0.00	*92→95	96%
		95→99	31%				
		95→100	30%				
29,912 (*30,800*)	0.33	95→98	39%	19,483 (*19,000*)	0.25	95→96	47%
		95→97	28%			*91→95	16%
		94→96	18%			94→96	12%
						*93→95	9%
30,513 (*33,900*)	0.24	95→97	28%	20,711 (*20,500*)	0.03	*91→95	77%
		95→98	20%			95→96	5%
		95→99	17%			94→96	5%
		95→100	12%				
32,262	0.01	95→100	47%	21,160 (*20,500*)	0.02	*90→95	93%
		95→99	39%				
		92→96	6%				
33,796	0.02	93→96	65%	22,945 (*22,000*)	0.08	94→96	50%
		90→96	13%			95→96	20%
						93→96	10%
34,941	0.01	90→96	56%	25,794	0.02	*89→95	59%
		92→96	27%			94→96	12%
		93→96	6%			95→97	8%

Transitions for **2**[·+], which are not present for **2** because of the doubly filled orbital (95) are denoted by an asterisk (*). Experimental data are given in parentheses.

With this relationship, a theoretical bandwidth of 2350 cm^{-1} can be calculated, which compares well with that one observed experimentally (2200 cm^{-1}).

3. Conclusions

The preparation of a 1,3-dithiol-2-ylidene substituted naphthopyrano compound has been demonstrated. The interpretation of the spectroscopic and cyclic voltammetric data on the basis of time-dependent density functional theory revealed that compound **2** acts as a donor–acceptor (D–A) system. The nature of the strong absorption band at 21,500 cm^{-1} (465 nm) could be assigned to a charge-transfer transition. The corresponding charge-transfer luminescence exhibits a large Stokes shift of 5800 cm^{-1}. Despite the low quantum efficiency of 0.5%, it represents a rare example of luminescence from such a D–A dyad. Therefore, the preparation of a naphthopyrano extended TTF or the attachment of 1,3-dithiol-2-ylidene units to NDA and perylenedicarboxylic anhydride is further investigated in expectation of interesting D–A properties.

4. Experimental

4.1. General considerations

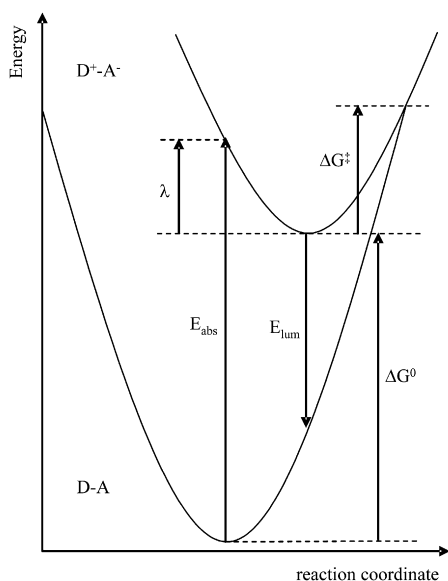The compound 4,5-ethylenedithio-1,3-dithiole-2-thione **1** was prepared according to the literature procedure.[21] All

Figure 7. Potential energy surface of a charge-transfer transition in the case of $D-A + E_{abs} \rightarrow D^+-A^-$. E_{abs}: optical transition energy, λ: reorganizational energy, ΔG^0: free energy term, $\Delta G^{\ddagger}$: dynamic thermal parameter.[20]

other chemicals and solvents were purchased from commercial sources and were used without further purification. Absorption spectra were recorded on a Cary 50 Bio UV–vis spectrophotometer and on a Bruker IFS66/S NIR spectrophotometer at room temperature. Emission and excitation spectra were measured on a Horiba Fluorolog 3. The solutions were degassed by bubbling nitrogen through them for 20 min before measuring. Compound **2** was measured as a CH_2Cl_2 solution and the oxidation agent $FeCl_3$ was added as a CH_3CN solution.

4.2. Synthesis

4.2.1. 3-(4,5-Ethylenedithio-1,3-dithiol-2-ylidene)-1*H*,3*H*-naphtho[1,8-*cd*]pyran-1-one (2).
Compound **1** (0.26 g, 1.2 mmol) and 1,8-naphthalic anhydride (0.15 g, 0.8 mmol) were suspended in 20 ml of dry toluene under N_2. Then, 1.8 ml of $P(OMe)_3$ was added and the yellowish suspension was refluxed for 3 h at 125 °C. The solvent was evaporated from the red mixture by distillation. Purification of the reddish brown solid by column chromatography eluting with a gradient of 0–100% EtOAc in CH_2Cl_2 yielded **2** as red solid. Yield: 0.15 g (54%). Crystals were grown by layer diffusion. A CH_2Cl_2 solution of **2** was superposed by a MeOH layer. Mp 230–233 °C. Anal. Calcd for $C_{17}H_{10}O_2S_4$: C, 54.52; H, 2.69. Found: C, 54.51; H, 2.82. ^{1}H NMR (CD_2Cl_2) δ: 3.30 (s, 4H), 7.29 (dd, J^1=7.4 Hz, J^2=0.8 Hz, 1H), 7.61 (t, J=7.8 Hz, 1H), 7.62 (t, J=7.7 Hz, 1H), 7.72 (d, J=7.9 Hz, 1H), 8.08 (dd, J^1=8.3 Hz, J^2=1.1 Hz, 1H), 8.28 (dd, J^1=7.3 Hz, J^2=1.1 Hz, 1H). ^{13}C NMR (THF-d_8) δ: 30.20, 30.38, 121.42, 123.57, 123.72, 126.49, 127.84, 128.15, 129.03, 129.64, 138.96, 134.60. IR (KBr, cm^{-1}): 3435, 2924, 1735, 1513, 1372, 1352, 1251, 1183, 1148, 1127, 1090, 829, 777, 763, 743, 518. MS (EI) m/z 374 (M$^+$).

4.3. X-ray crystallography

An orange rod-like crystal of compound **2** was mounted on a Stoe Mark II-Imaging Plate Diffractometer System[22]

equipped with a graphite-monochromator. Data collection were performed at -100 °C using Mo Kα radiation (λ=0.71073 Å). One hundred and twenty exposures (6 min per exposure) were obtained at an image plate distance of 135 mm, φ=0° and 0°<ω<180° with the crystal oscillating through 1.5° in ω. The resolution was $D_{min}-D_{max}$ 23.99$-$0.82 Å. The structure was solved by direct methods using the program SHELXS-97[23] and refined by full matrix least squares on F^2 with SHELXL-97.[24] All hydrogen atoms were included in calculated positions and treated as riding atoms using SHELXL-97 default parameters. All non-hydrogen atoms were refined anisotropically. An empirical absorption correction was applied using DELrefABS (PLATON03,[25] T_{min}=0.168, T_{max}=0.640). Crystal data have been deposited at the Cambridge Crystallographic Data Centre, reference CCDC 612152. Copy of the data can be obtained, free of charge, on application to CCDC, 12 Union Road, Cambridge CB2 1EZ, UK [fax: +44 1223 336033 or e-mail: deposit@ccdc.cam.ac.uk].

4.4. Computational details

Electronic excitation energies and absorption intensities of the neutral and of the singly ionized form of **2** have been computed using the program package ORCA.[16] The hybrid B3LYP functional and both Ahlrichs valence double zeta (VDZ)[13] and, alternatively for comparison, triple-zeta (TZV) basis sets,[14] and polarization functions[15] have been utilized along with the ORCA implementation of the time-depending DFT method.[17] Excitation energies have been computed both with the experimental geometry of the neutral **2** and with B3LYP optimized geometries of the neutral **2**, and the singly ionized gas phase species **2**$^{\bullet+}$.

Supplementary data

Supplementary data associated with this article can be found in the online version, at doi:10.1016/j.tet.2006.09.032.

References and notes

1. (a) Law, K.-Y. *Handbook of Organic Conductive Molecules and Polymers*; Nalwa, H. S., Ed.; Wiley: Chichester, UK/ New York, NY, 1997; Vol. 1, Chapter 10; (b) Tang, C. W. *Appl. Phys. Lett.* **1986**, *48*, 183–185; (c) Iqbal, Z.; Ivory, M.; Eckhardt, H. *Mol. Cryst. Liq. Cryst.* **1988**, *158B*, 337–352; (d) Wüsten, J.; Berger, S.; Heimer, K.; Lach, S.; Ziegler, Ch. *J. Appl. Phys.* **2005**, *98*, 013705.
2. (a) Heywang, G.; Born, L.; Fitzky, H.-G.; Hassel, T.; Hocker, J.; Müller, H.-K.; Pittel, B.; Roth, S. *Angew. Chem., Int. Ed. Engl.* **1989**, *28*, 483–485; (b) Hoier, H.; Zacharias, D. E.; Carrell, L.; Glusker, J. P. *Acta Crystallogr., Sect. C* **1993**, *49*, 523–526; (c) Zacharias, D. E. *Acta Crystallogr., Sect. C* **1993**, *49*, 1082–1087.
3. Almeida, M.; Henriques, R. T. *Handbook of Organic Conductive Molecules and Polymers*; Nalwa, H. S., Ed.; Wiley: Chichester, UK/New York, NY, 1997; Vol. 1, Chapter 2.

4. Special issue on molecular conductors: *Chem. Rev.* **2004**, *104*, 4887; Batail, P., Ed.

5. *TTF Chemistry: Fundamentals and Applications of Tetrathiafulvalene*; Yamada, J., Sugimoto, T., Eds.; Springer: Berlin, 2004.

6. (a) Ho, G.; Heath, J. R.; Kondratenko, M.; Perepichka, D. F.; Arseneault, K.; Pézolet, M.; Bryce, M. R. *Chem.—Eur. J.* **2005**, *11*, 2914–2922; (b) Tsiperman, E.; Becker, J. Y.; Khodorkovsky, V.; Shames, A.; Shapiro, L. *Angew. Chem., Int. Ed.* **2005**, *44*, 4015–4018; (c) Bendikov, M.; Wudl, F.; Perepichka, D. F. *Chem. Rev.* **2004**, *104*, 4891–4946.

7. Leroy-Lhez, S.; Baffreau, J.; Perrin, L.; Levillain, E.; Allain, M.; Blesa, M.-J.; Hudhomme, P. *J. Org. Chem.* **2005**, *70*, 6313–6320.

8. (a) Guo, X.; Zhang, D.; Huijuan, Z.; Fan, Q.; Xu, W.; Ai, X.; Fan, L.; Zhu, D. *Tetrahedron* **2003**, *59*, 4843–4850; (b) Guo, X.; Gan, Z.; Luo, H.; Araki, Y.; Zhang, D.; Zhu, D.; Ito, O. *J. Phys. Chem. A* **2003**, *107*, 9747–9753; (c) Guo, X.; Zhang, D.; Xu, W.; Zhu, D. *Synth. Met.* **2003**, *137*, 981–982.

9. O'Neil, M. P.; Niemcyk, M. P.; Svec, W. A.; Gosztola, D.; Gaines, L. L.; Wasielewski, M. R. *Science* **1992**, *257*, 63–65.

10. (a) Frère, P.; Skabara, P. *Chem. Soc. Rev.* **2005**, *34*, 69–98; (b) Takahashi, K.; Ise, T.; Mori, T.; Mori, H.; Tanaka, S. *Chem. Lett.* **1998**, 1147–1148; (c) Takahashi, K.; Ise, T. *Heterocycles* **1997**, *45*, 1051–1054; (d) Ise, T.; Takahashi, K. *J. Cryst. Growth* **2001**, *229*, 591–594.

11. Farrugia, L. J. *J. Appl. Crystallogr.* **1997**, *30*, 565. ORTEP-3 for Windows.

12. Grigor'eva, L. P.; Chetkina, L. A. *Kristallografiya* **1975**, *20*, 1289–1290.

13. Schäfer, A.; Horn, H.; Ahlrichs, R. *J. Chem. Phys.* **1992**, *97*, 2571–2577.

14. Schäfer, A.; Huber, C.; Ahlrichs, R. *J. Chem. Phys.* **1994**, *100*, 5829–5835.

15. Ahlrichs, R., and co-workers, unpublished, available from: ftp://ftp.chemie.uni-karlsruhe.de/pub/BASES/Def or ftp://ftp.chemie.uni-karlsruhe.de/pub/BASES/Def2, respectively.

16. Neese, F. *ORCA – An Ab initio, DFT and Semiempirical SCF-MO-Package, Version 2.4–41*; Max-Planck-Institut für Bioanorganische Chemie: Mühlheim/Ruhr, Germany, October 2005.

17. Neese, F.; Olbrich, G. *Chem. Phys. Lett.* **2002**, *362*, 170–178.

18. (a) Hush, N. S. *Prog. Inorg. Chem.* **1967**, *8*, 391–443; (b) Marcus, R. A. *Angew. Chem., Int. Ed. Engl.* **1993**, *32*, 1111–1121.

19. Bernhardt, P. V.; Bozoglián, F.; Macpherson, B. P.; Martínez, M. *Coord. Chem. Rev.* **2005**, *249*, 1902–1916.

20. Bernhardt, P. V.; Martinez, M. *Inorg. Chem.* **1999**, *38*, 424–425.

21. Svenstrup, N.; Becher, J. *Synthesis* **1995**, *3*, 215–235.

22. Stoe and Cie. *X-Area V1.17 & X-RED32 V1.04 Software*; Stoe und Cie GMBH: Darmstadt, Germany, 2002.

23. Sheldrick, G. M. *Acta Crystallogr., Sect. A* **1990**, *46*, 467–473.

24. Sheldrick, G. M. *SHELXL-97: Program for Crystal Structure Refinement*; University of Göttingen: Göttingen, Germany, 1997.

25. Spek, A. L. *J. Appl. Crystallogr.* **2003**, *36*, 7–13.